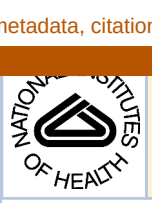

Published in final edited form as:
Cancer Res. 2009 March 15; 69(6): 2479–2486. doi:10.1158/0008-5472.CAN-08-4152.

Molecular dosimetry of 1, 2, 3, 4-diepoxybutane induced DNA-DNA crosslinks in B6C3F1 mice and F344 rats exposed to 1,3-butadiene by inhalation

Melissa Goggin,
Masonic Cancer Center and Department of Medicinal Chemistry, University of Minnesota, Minneapolis, MN 55455

James A. Swenberg,
University of North Carolina at Chapel Hill, Chapel Hill, North Carolina 27599

Vernon E. Walker, and
Lovelace Respiratory Research Institute, Albuquerque, New Mexico 87108

BioMosaics, Inc., Burlington, VT 05405

Natalia Tretyakova*
Masonic Cancer Center and Department of Medicinal Chemistry, University of Minnesota, Minneapolis, MN 55455

Abstract

1,3-butadiene (BD) is an important industrial and environmental chemical classified as a human carcinogen based on epidemiological studies in occupationally exposed workers and animal studies in laboratory rats and mice. BD is metabolically activated to three epoxides that can react with nucleophilic sites in biomolecules. Among these, 1,2,3,4-diepoxybutane (DEB) is considered the ultimate carcinogen due to its high genotoxicity and mutagenicity attributed to its ability to form DNA-DNA crosslinks. Our laboratory has developed quantitative HPLC-μESI$^+$-MS/MS methods for two DEB-specific DNA-DNA cross-links, 1,4-*bis*-(guan-7-yl)-2,3-butanediol (*bis*-N7G-BD) and 1-(guan-7-yl)-4-(aden-1-yl)-2,3-butanediol (N7G-N1A-BD). This report describes molecular dosimetry analysis of these adducts in tissues of B6C3F1 mice and F344 rats exposed to a range of BD concentrations (0–625 ppm). Much higher (4–10-fold) levels of DEB-DNA cross-links were observed in mice as compared to rats exposed to the same BD concentrations. In both species, *bis*-N7G-BD levels were 1.5–4 fold higher in the liver than in other tissues examined. Interestingly, tissues of female animals exposed to BD contained higher concentrations of *bis*-N7G-BD adducts than tissues of male animals, which is in accord with previously reported differences in tumor incidence. The molecular dosimetry data presented herein suggests that species and gender differences observed in BD-induced cancer are directly related to differences in the extent of BD metabolism to DEB. Furthermore, a rat model of sensitivity to BD may be more appropriate than a mouse model for assessing human risk associated with BD exposure, since rats and humans appear to be similar in respect to DEB formation.

Keywords

1,3-butadiene; DNA-DNA crosslinks; interspecies differences; metabolism; mass spectrometry

*Corresponding author: 760E CCRB, Univ. of Minnesota Cancer Center, 806 Mayo, 420 Delaware St. S.E., Minneapolis, MN 55455; Tel. (612) 626-3432; Fax: (612) 626-5135; trety001@umn.edu.

Introduction

1,3-Butadiene (BD) is a high volume industrial chemical used in the production of plastics and rubber (1). It is also an environmental toxin present in automobile exhaust and in cigarette smoke (2,3). BD is classified as a human carcinogen based on laboratory animal data linking it to the formation of tumors, human epidemiology data revealing increased incidence of leukemia and lymphohematopoietic cancers in occupationally exposed workers, and genotoxicity data for laboratory animals demonstrating the induction of point mutations, large deletions, and chromosomal aberrations following exposure to BD (4–8). Due to the ubiquitous human exposures to BD, there is a pressing need to identify biomarkers of BD exposure for use in quantitative risk assessment. In particular, specific biomarkers of the metabolic activation of BD to DNA-reactive intermediates are required.

BD is metabolized by cytochrome P450 monooxygenases to generate three reactive epoxides, e.g. 3,4-epoxybutene (EB), 3,4-epoxy-1,2-butanediol (EBD), and 1,2,3,4-diepoxybutane (DEB) (Figure 1) (9–11). Although all three epoxide metabolites can react with DNA, DEB is considered the ultimate carcinogenic form of BD because of its potent genotoxicity and its ability to form bifunctional DNA adducts such as DNA-DNA cross-links and exocyclic DNA lesions (12–14). Studies in human cell culture reveal that DEB is 100–200-fold more mutagenic than BD-derived epoxides that possess a single epoxide functionality (15). DEB preferentially alkylates the N7 position of guanine bases in DNA to form N7-(2'-hydroxy-3', 4'-epoxybut-1'-yl)-guanine (N7-HEB-dG) adducts (16). The epoxide group of N7-HEB-dG can then be hydrolyzed to N7-(2’, 3’, 4’-trihydroxybut-1’-yl)-guanine (THBG), or, less frequently, can react with another site in DNA, such as the N7 of another guanine or the N1 of an adenine (13,17). The latter reaction forms 1,4-*bis*-(guan-7-yl)-2,3-butanediol *(bis*-N7G-BD) and 1-(guan-7-yl)-4-(aden-1-yl)-2,3-butanediol (N7G-N1A-BD) cross-links (Figure 1) (13,17). Alkali-catalyzed Dimroth rearrangement of N7G-N1A-BD leads to the corresponding N7G-N^6A-BD adducts (Figure 1) (18).

Chronic BD inhalation studies in mice and rats revealed that it was carcinogenic in both species, but with a striking difference in sensitivity and tissue specificity. Mice developed tumors following exposure to as low as 6.25 ppm BD (8), whereas in rats, tumors were not observed until the exposure reached 1000 ppm BD (19). Furthermore, the target tissues for BD-induced cancer in mice (lung, heart, hematopoietic system) were different from those in rats (thyroid, pancreas, testis, uterus) (8,19). The increased susceptibility of mice to the carcinogenicity of BD may result from a more efficient metabolic activation of BD to DEB in this species (20–22). Indeed, several studies have found that target tissues of BD-exposed mice, especially lung, contain significant levels of DEB (23). DEB-specific *N*,*N*-(2,3-dihydroxy-1,4-butanediyl)-valine (*pyr*-Val) globin adducts were detected in mice treated with as little as 3 ppm BD by inhalation (24). In contrast, the formation of DEB in rat tissues is negligible, providing a possible explanation for the weak tumorigenic response to BD in this species (22–25). Consistent with this model, rat, mouse, and human cells are equally sensitive to the genotoxic effects of DEB when it is introduced directly into isolated lymphocytes (26,27). However, the formation of DEB-specific DNA-DNA adducts in tissues of laboratory mice and rats exposed to BD has not been previously investigated.

Earlier studies analyzed DEB monoadducts in rodent tissues in an attempt to explain the observed interspecies differences in carcinogenic response. Koc et al. examined the formation of THBG adducts (Figure 1) in the liver DNA of B6C3F1 mice and F344 rats treated with 62.5–625 ppm of BD for 4 weeks (28). THBG levels were only 2-fold higher in mice than in rats (28) and thus are unlikely to account for the 1000-fold greater sensitivity of mice to BD-mediated cancer. The study concluded that over 95% of the THBG adducts were formed not

from DEB, but from another, more prevalent metabolite of BD, 3,4-epoxy-1,2-butanediol (EBD) (Figure 1) (28). These results emphasized the need for a unique biomarker for DEB to use in predicting the carcinogenic risk of BD (28,29).

We have recently developed a quantitative HPLC-ESI-MS/MS methodology for two types of DEB-specific DNA-DNA cross-links, 1,4-*bis*-(guan-7-yl)-2,3-butanediol (*bis*-N7G-BD) and 1-(guan-7-yl)-4-(aden-1-yl)-2,3-butanediol (N7G-N1A-BD) (18,30). In our approach, the cross-linked nucleobases are released from the DNA backbone by neutral thermal or mild acid hydrolysis, enriched by ultrafiltration and HPLC or solid phase extraction, and analyzed by capillary HPLC-ESI-MS/MS using the corresponding ^{15}N-labeled adducts as internal standards (18,30). The N7G-N1A-BD adducts are converted to the corresponding 1-(guan-7-yl)-4-(aden-6-yl)-2,3-butanediol (N7G-N^{6}A-BD) lesions *via* forced Dimroth rearrangement prior to analysis in order to improve the sensitivity of the method and to eliminate adduct decomposition during sample processing (18). We found that liver DNA of female C57BL/6 and B6C3F1 mice exposed to 625 ppm BD by inhalation contained *bis*-N7G-BD adducts in ten fold greater amounts than N7G-N1A-BD (18,30). However, unlike *bis*-N7G-BD cross-links which are hydrolytically labile and are spontaneously released from DNA by depurination ($t_{1/2}$, 81.5 h), N7G-N1A-BD lesions may persist in DNA and accumulate in tissues over time (13,18).

The objective of the present work was to quantify DEB-induced DNA-DNA cross-links in tissues of laboratory rats and mice exposed to BD by inhalation in an attempt to establish the structural basis of species differences in sensitivity to BD-mediated carcinogenesis and mutagenesis. We obtained dose-response relationships for DEB-induced DNA-DNA cross-links in tissues of B6C3F1 mice and F344 rats exposed to increasing concentrations of BD (6.25, 62.5, 200, and 625 ppm for 2 weeks). Unlike previous results for THBG adducts (28), the amounts of DEB-specific bifunctional DNA adducts exhibited important interspecies and gender differences which correlate with previously observed differences in tumorigenic susceptibility, supporting the idea that DEB plays an important role in BD-mediated cancer in mice.

Materials and Methods

Note: DEB is a known carcinogen and must be handled with adequate safety precautions.

Materials and Methods

All chemicals and solvents were obtained from Sigma-Aldrich (Milwaukee, WI), unless stated otherwise. Racemic and *meso bis*-N7G-BD, [$^{15}N_{10}$]-*bis*-N7G-BD N7G-N1A-BD, and [$^{15}N_3$,$^{13}C_1$]-N7G-N1A-BD were prepared in our laboratory as described elsewhere (18,31).

Animals and treatment

Animals (B6C3F1 mice and F344 rats) were randomly separated into air-control and exposure groups by weight and were housed individually in hanging wire stainless steel cages according to NIH guidelines (NIH Publication 86-23, 1985). All procedures involving the use of animals were approved by the Institutional Animal Care and Use Committee. Experimental animals were exposed using multitiered whole body exposure chambers (H-2000, Laboratory Products, Aberdeen, MD). Rodents in one chamber received filtered air only as a control group, and rodents in the other chamber received nominal 6.25, 62.5, 200, or 625 ppm BD for 2 weeks (6 h/day, 5 days/week). Animals were housed within exposure chambers throughout the experiment and had free access to food and water except for removal of food during the 6 h exposure periods. Within 2 h after cessation of the final day of exposure, animals were euthanized via cardiac puncture, and tissues were harvested and snap-frozen for storage at −80

°C. Tissues were shipped on dry ice to the University of Minnesota where they were stored at −80 °C until DNA extraction.

DNA isolation

DNA was isolated using NucleoBond AXG500 anion exchange cartridges (Macherey-Nagel Bethlehem, PA) according to manufacturer's procedures. In brief, tissues (0.1 – 0.4 g) were homogenized and incubated with RNAse and proteinase K at 50 °C for 2–4 hours. Samples were loaded on NucleoBond AXG cartridges, which were prepared and washed following the kit instructions. Following elution, DNA was precipitated by the addition of isopropanol. The DNA was spooled, washed 3 times with cold 70% ethanol, dried, and dissolved in Milli-Q water (500 µL). DNA purity and amounts were determined by UV spectrophotometry. Typical A_{260}/A_{280} ratios were between 1.7 and 1.9, ensuring minimal protein contamination.

Bis-N7G-BD sample preparation

DNA (100 µg) was dissolved in 200 µL of water, spiked with racemic and *meso* $^{15}N_{10}$- *bis*-N7G-BD internal standards (300 fmol each) and heated at 70 °C for 1 hour to release N7-alkylguanine adducts. Following thermal hydrolysis, the partially depurinated DNA backbone was removed by ultrafiltration with Centricon YM-10 filters (Millipore Corp., Billerica, MA). The filtrates containing *bis*-N7G-BD were further purified by offline HPLC as described below, while partially depurinated DNA was recovered for future analysis of N7G-N1A-BD (see below) (18). Offline HPLC purification of *bis*-N7G-BD was performed using a Zorbax Eclipse XDB-C18 (4.6 × 150 mm, 5 µm) column. *Bis*-N7G-BD was eluted with a gradient consisting of 0.4% formic acid in H_2O (A) and acetonitrile (B). The column was maintained at 0% B for 5 minutes, followed by a linear increase to 3% B in 10 minutes, and then further to 40% B over 5 minutes. The system was equilibrated for 15 minutes between runs. The retention time of *bis*-N7G-BD (12.4 minutes) was determined with $^{15}N_{10}$-labeled internal standard to prevent carryover contamination. Samples were spiked with 2'-deoxythymidine (retention time 9.8 min) and 2'-deoxyadenosine (retention time 16.6 min) (0.5 µg each) as HPLC retention time markers. HPLC fractions containing *bis*-N7G-BD were dried under vacuum and reconstituted in 0.05 % acetic acid (25 µL) prior to LC-MS/MS analysis.

N7G-N1A-BD sample preparation

Partially depurinated DNA backbone recovered from neutral thermal hydrolysis was spiked with $^{13}C_1$,$^{15}N_3$-N7G-N1A-BD (300 fmol, internal standard for mass spectrometry) and hydrolyzed in the presence of 0.1 M HCl to release all purine bases, including N7G-N1A-BD. The hydrolysates were filtered by YM-10 filters and purified by solid phase extraction on C18 cartridges as previously reported (18). Samples were heated in base (1.0 M NH_4OH at 70 °C for 16 h) to force Dimroth rearrangement of N7G-N1A-BD to N7G-N^6A-BD (18). The ammonium hydroxide was removed under vacuum, and samples were dissolved in 0.05% acetic acid (25 µL) prior to LC-MS/MS analysis.

HPLC-µESI$^+$-MS/MS

MS instrumentation and chromatographic separation of *bis*-N7G-BD was achieved using previously published methods (30), with minor changes to HPLC conditions to improve sensitivity. Our optimized method utilizes 0.05% acetic acid (A) and methanol (B) as HPLC solvents. A Zorbax Extend C18 column (3.5 µm, 150 × 0.5 mm) was eluted with a gradient of 0 to 10 % B in 5 minutes, further from 10% to 60% over 10 minutes, and ramped back to 0% B over 3 minutes. The HPLC flow rate was 10 µL/min, the column temperature was maintained at 40 °C, and the injection volume was typically 8 µL. With this solvent system, the retention time of racemic *bis*-N7G-BD was 9.9 min, while *meso bis*-N7G-BD eluted at 10.9 min.

UPLC-nanoESI-MS/MS analysis of N7G-N^{6}A-BD

A Waters nanoAquity UPLC system (Waters Corp., Millford, MA) interfaced to a Thermo-Finnigan TSQ Quantum Ultra mass spectrometer (Thermo Fisher Scientific Corp., Waltham, MA) was used for these analyses. HPLC solvents were 0.01% acetic acid in water (A) and 1:1 LC-MS grade methanol/acetonitrile (B). Samples (4–8 μL) were loaded on a trapping column (Symmetry C18 nanoAcquity 0.18 × 20 mm) for 1 min at 0% B. Chromatographic separation was achieved using an Atlantis C18 (75 × 100 μm, Waters) column eluted at a flow rate of 0.350 μL/min. A linear gradient program was employed as follows: from 0 to 12 % B in 2 minutes, further to 25% B over 7 minutes, and finally to 45% B over 15 minutes. The column was equilibrated at 0% B for at least 12 minutes before each run. Under these conditions, both racemic and *meso* N7G-N^{6}A-BD eluted at 16.9 minutes. The mass spectrometer was operated in the selected reaction monitoring (SRM) mode by following mass transitions corresponding to the neutral loss of guanine from protonated molecules of the adduct: *m/z* 373.1 → *m/z* 222.1 $[M + H - Gua]^+$ (N7G-N^{6}A-BD) and *m/z* 377.1 → *m/z* 222.1 $[M + H - [^{13}C_1,^{15}N_3]Gua]^+$ ($^{13}C_1,^{15}N_3$-N7G-N^{6}A-BD) (18).

N7G-N1A-BD method validation

Three replicates of control mouse liver DNA (partially depurinated and collected from YM-10 filters) were spiked with N7G-N1A-BD (1 fmol) and internal standard (300 fmol). The validation samples were processed (by acid hydrolysis, filtration, SPE, and forced Dimroth rearrangement) following the same methods as real samples. The validation samples were each analyzed on three separate days to determine accuracy and precision of the methods.

Statistical analysis

Statistical analyses were performed using Microsoft Excel spreadsheet analysis tools. A student's t-test (2 sample assuming unequal variances) was used to determine p-values for female/male differences in adduct levels.

Results

Optimization and validation of HPLC-MS/MS methods

The capillary HPLC-ESI$^+$-MS/MS methods for *bis*-N7G-BD and N7G-N1A-BD previously developed in our laboratory (18,30) were not sensitive enough to quantify DEB-specific DNA-DNA cross-links in tissues of laboratory mice and rats exposed to low concentrations of BD. Therefore, both methods were further optimized to improve sensitivity and reproducibility. The assay for *bis*-N7G-BD was optimized by incorporating an off-line HPLC clean-up step instead of solid phase extraction. In addition, the solvent system for capillary HPLC-ESI$^+$-MS/MS analysis was changed from ammonium acetate buffer/ACN to water/methanol. With these modifications, the limit of quantitation (LOQ) was improved from 10 fmol/100 μg DNA to 2 fmol/100 μg mouse liver DNA (or 6 *bis*-N7G-BD/10^9 nts). The quantitative methods for N7G-N1A-BD were optimized by incorporating nanospray HPLC-ESI$^+$-MS/MS, leading to an improved LOQ from 5 fmol/100 μg DNA to 1 fmol/100 μg DNA (or 3 N7G-N1A-BD/10^9 nts). The optimized methods were validated by analyzing control DNA samples spiked with known amounts of analyte and internal standard. Intraday accuracy and precision of 91% ± 14% were observed for 1 fmol N7G-N1A-BD spiked into control mouse liver DNA (Full validation data and representative nanospray-MS/MS chromatogram can be found in Supplemental Information, S-1 and S-2).

Because all three stereoisomers of DEB are formed metabolically (*R,R*; *S,S*; and *meso* DEB) (11), three stereoisomers of the DEB-DNA cross-links can potentially be formed (Figure 1). Our current methods analyze *R,R* and *S,S bis*-N7G-BD isomers as a racemic mixture separate

from *meso bis*-N7G-BD. N7G-N1A-BD adducts are converted to the corresponding N7G-N^6A-BD adducts by forced Dimroth rearrangement (Figure 1), because our previous studies demonstrated that this results in a greater sensitivity for *in vivo* sample analyses (18). Based on our *in vitro* studies, N7G-N1A-BD is the most abundant Gua-Ade cross-link of DEB, while little N7G-N^6A-BD is formed at concentrations below 500 μM DEB (17,18). Therefore, the majority of N7G-N^6A-BD adducts being measured by our methods represent N7G-N1A-BD lesions formed *in vivo*.

Dose Response Curves

The optimized HPLC-ESI^+-MS/MS methods described above were used to quantify *bis*-N7G-BD and N7G-N1A-BD/N7G-N^6A-BD cross-links in liver DNA of B6C3F1 mice and F344 rats exposed to a range of BD concentrations (0 to 625 ppm) by inhalation for 10 days (Figure 2 and Figure 3). We found that *S,S* + *R,R* (racemic) *bis*-N7G-BD was the most abundant DNA cross-link formed upon exposure to BD in both species, followed by *meso bis*-N7G-BD and N7G-N1A-BD/N7G-N^6A-BD. The molar ratio of G-G and G-A DEB cross-links observed in current work (~ 10:1) is consistent with a lower reactivity of adenine nucleobases towards epoxide electrophiles (32) and is similar to the molar ratios of N7-(2',3',4'-trihydroxybut-1'-yl)guanine (N7-THBG) and N^6-(2',3',4'-trihydroxybut-1'-yl)adenine (N^6-THBA) monoadducts reported previously (33,34).

Significant interspecies differences were observed between DEB-DNA adduct levels in mouse and rat DNA (Figure 2). Concentrations of racemic *bis*-N7G-BD were 4–10 fold higher in mice than in rats at all exposure levels. While the shape of the *bis*-N7G-BD dose response curve for mice appears curvilinear, bending downward slightly between 6.25 and 625 ppm BD, rat adduct levels reached a plateau at 62.5 ppm, suggesting that the metabolic activation of EB to DEB is saturated in this species (Figure 2). The only DEB-DNA crosslink observed at the lowest BD exposure (6.25 ppm) in mice was *S,S*+ *R,R bis*-N7G-BD (0.32 ± 0.09 adducts/10^7 nts). The lowest exposure at which measurable levels of *bis*-N7G-BD were observed in rats was 62.5 ppm, although we did not have access to tissues of animals exposed to BD amounts between 6.25 and 62.5 ppm.

A similar trend was observed for N7G-N1A-BD/N7G-N^6A-BD, which was significantly more abundant in liver DNA of mice as compared to the corresponding rat tissue (Figure 3). The dose response curve for N7G-N1A-BD/N7G-N^6A-BD is much steeper in the mouse than in the rat, which exhibits signs of metabolic saturation at exposures above 62.5 ppm BD (Figure 3). These results are fully consistent with the data for *bis*-N7G-BD (Figure 2).

Tissue distribution of bis-N7G-BD

To analyze the tissue distribution of DEB-DNA adducts following exposure of laboratory mice and rats to BD by inhalation, *bis*-N7G-BD adduct levels were determined in liver, lung, kidney, brain, and thymus tissues. In both species, *bis*-N7G-BD levels were highest in the liver (Table 1). For BD-exposed mice, liver adduct levels (3.95 *S,S* + *R,R bis*-N7G-BD/10^7 nts) were about 3 fold higher than in the other tissues (0.38 – 1.35 *S,S* + *R,R bis*-N7G-BD/10^7 nts) (Table 1). In BD-exposed rats, liver adduct levels (0.36 *S,S* + *R,R bis*-N7G-BD/10^7 nts) were ~1.5 fold higher than in the other tissues (0.21 – 0.30 *S,S* + *R,R bis*-N7G-BD/10^7 nts) (Table 1).

Gender differences in DEB-DNA adduct formation

Female mice develop tumors at lower BD exposure than males, indicating gender differences in susceptibility (15). It has been previously reported that when exposed to 62.5 ppm BD for 6 h, the concentration of DEB in the blood of female rats is 6 fold greater than in males (22). Similarly, the formation of DEB-specific globin adducts (*N,N*-(2,3-dihydroxy-1,4-butanediyl)-valine, *pyr*-Val) is 2–4 fold higher in female than in male rats exposed to 1,000 ppm BD (24).

Therefore, we investigated potential gender differences in the formation of *bis*-N7G-BD adducts in the liver DNA of female and male mice and rats exposed to 625 ppm BD (Figure 4). We found that in both species, the amounts of *S,S, R,R bis*-N7G-BD were 2 – 2.5 fold higher in female animals as compared to males subjected to the same exposure conditions. Furthermore, the amounts of *meso bis*-N7G-BD adducts were 3-fold higher in female mouse liver DNA than the corresponding amounts in male mouse liver DNA (data not shown). Tissues were not available for full dose response analyses in male animals; however, similar gender differences were observed in animals exposed to 200 ppm BD (Figure 4).

Discussion

Although BD is a known mutagen and carcinogen present ubiquitously in urban air, the exact mechanisms of its mutagenic and carcinogenic activity remain to be established. Furthermore, human BD exposure risk assessment is complicated by large interspecies differences in sensitivity to BD-induced cancer. BD is a potent carcinogen in mice, but is only a weak carcinogen in rats. B6C3F1 mice develop tumors at BD exposure concentrations three orders of magnitude lower than those that cause cancer in Sprague-Dawley rats (19,22,23). It has been proposed that the carcinogenic potency of BD in a given organism can be predicted from the relative amount of the diepoxide metabolite, DEB, generated upon metabolic activation (27, 29). However, *in vivo* formation and repair of bifunctional DEB-DNA adducts in laboratory rats and mice exposed to BD have not been previously investigated.

We have developed sensitive and specific HPLC-ESI-MS/MS methods which, for the first time, quantify the formation of DEB-specific DNA adducts *in vivo* following inhalation exposure to BD. Our results for dose-dependent formation of *bis*-N7G-BD and N7G-N1A-BD/N7G-N^6A-BD in tissues of laboratory mice and rats exposed to 0–625 ppm BD by inhalation (Figure 2 and Figure 3) reveal remarkable interspecies differences between adduct levels. For example, the concentrations of *bis*-N7G-BD adducts in mouse liver following 10 day exposure to 625 ppm BD were 10-fold greater than in rats exposed at the same conditions (Figure 2). Both *bis*-N7G-BD and N7G-N1A-BD/N7G-N^6A-BD reach a plateau in rat after inhalation exposures above 62.5 ppm, possibly a result of enzymatic saturation, P450 2E1 inactivation through phosphorylation (35), or suicide inhibition of the protein by covalent binding of epoxide products to the active site (36). These results are consistent with a greater sensitivity of laboratory mice to BD-mediated carcinogenesis (8,19), suggesting that DEB-induced bifunctional DNA lesions play an important role in BD-mediated cancer.

Our results are in accord with previously published dose response data for DEB-specific hemoglobin adducts (*pyr*-Val), which revealed that DEB adduct levels in mice were 4–10× greater than levels in rats exposed to the same conditions (37). The dose response curves for both DEB-induced hemoglobin adducts (37) and DNA-DNA cross-links (Figure 2 and Figure 3 of the current manuscript) in the rat are supralinear, providing evidence for the saturation of metabolic activation pathways in this species following exposure to 62.5 ppm BD (38). In contrast, the dose response curves for the formation of DEB-specific DNA adducts in the mouse are curvilinear between 6.25 to 625 ppm BD, and do not show any signs of metabolic saturation (Figure 2 and Figure 3).

Taken together, these results suggest that the interspecies differences in the carcinogenic potency of BD in rats and mice are related to metabolic differences (11). Mice form 5-fold more DEB than rats per unit of BD exposure (39), which is reflected in a higher efficiency for the formation of DEB-globin adducts (37) and DEB-DNA adducts in this species (Table 2). As demonstrated in Table 2, the number of *bis*-N7G-BD adducts per BD exposure level in mice is greatest following a low BD exposure, but exceeds the efficiency of DEB-mediated DNA cross-linking in the rat at all BD exposures examined.

In addition to significant differences in sensitivity to BD carcinogenesis, rats and mice also differ in tissue specificity of BD-mediated tumor formation. In long-term inhalation studies, mice developed tumors of the lung, lymphatic system, liver, forestomach, and heart, while rats exhibited tumors in different tissues, including pancreas, testis, mammary gland, and thyroid gland (7). Our results presented in Table 1 indicate that these differences are not a result of tissue-dependent generation/accumulation of DEB. In both species, DEB-DNA adduct levels were highest in the liver (Table 1), consistent with the high activity of cytochrome P450 enzymes which activate BD to DEB in this tissue. *Bis*-N7G-BD concentrations in extrahepatic tissues (lung, kidney, brain, and thymus) were 1.5–3-fold lower than those in liver DNA, but similar to one another. These results are consistent with a model in which DEB is formed primarily in the liver and is transported throughout the body to reach other tissues (22).

Several recent studies suggested that there may be gender differences in cancer susceptibility and BD metabolism in laboratory animals. In carcinogenesis studies on BD, female mice develop tumors at lower BD concentrations than males (15). Furthermore, female rats contained higher blood DEB concentrations than male rats following a single 6 h exposure to 62.5 ppm BD (22). Female rats also had 3–4 fold greater levels of *pyr*-Val hemoglobin adducts than male rats following a 90 day exposure to 1000 ppm BD (24). Our results presented here are consistent with these earlier findings. *Bis*-N7G-BD adduct amounts in female rats and mice exposed to 625 ppm BD are 2–2.5-fold higher than in males (Figure 4). A similar trend is observed following lower BD exposure (200 ppm, Figure 4). In contrast, human epidemiology studies comparing male and female industry workers exposed to BD observed no significant difference in gene mutations (e.g., *HPRT* mutant frequencies) or sister chromatid exchanges between male and female workers (40,41). Future studies of DNA and protein adducts in occupationally exposed humans are needed to determine whether gender differences in biomarker levels of BD exposure and metabolism are observed in humans.

The possible roles of *bis*-N7G-BD and N7G-N1A-BD/N7G-N^6A-BD lesions investigated in the present work in the genotoxicity of DEB remain to be established. Several laboratories, including our group, have shown that *bis*-N7G-BD cross-links are formed preferentially within the 5'-GNC sequence context (31,42,43), with nucleosome structure having little effect on sequence selectivity of DEB-DNA cross-link formation (43). Interestingly, while the *S,S* stereoisomer of DEB produces a greater number of interstrand cross-links, all three DEB stereoisomers target 5'-GNC trinucleotides (44). Large local distortions of the DNA helix are required to accommodate 1,3-interstrand *bis*-N7G-BD lesions because the four-carbon tether length (6 Å) is much shorter than the spacing between the distal N7-dG atoms in 5'-GNC sequences of canonical B-DNA (8.9 Å). In addition, *meso* DEB is capable of inducing 1,2-intrastrand *bis*-N7G-BD lesions (31). Molecular dynamics simulations predict that the base stacking and hydrogen bonding interactions in the vicinity of 1,3-interstrand and 1,2-intrastrand *bis*-N7G-BD cross-links are disrupted as a result of twisting of the cross-linked residues with respect to the base-pairing plane (31). 3'-Exonuclease activity of *E. coli* Polymerase I is blocked one nucleotide ahead of the interstrand *bis*-N7G-BD lesions (31), consistent with an induced structural change in the vicinity of the cross-link. These structural changes may be important for the recognition of *bis*-N7G-BD adducts by DNA repair enzymes.

Another factor that must be considered when evaluating possible contributions of *bis*-N7G-BD and N7G-N1A-BD cross-links to BD-mediated mutagenesis and cancer is differences in their hydrolytic stability. All N7-alkylguanine adducts are hydrolytically labile because of the intrinsic destabilization of the glycosidic bond when the N7 position of guanine is alkylated (45). Both glycosidic bonds of *bis*-N7G-BD cross-links can be hydrolyzed, with a half-life in double stranded DNA of 147 h (interstrand) and 35 h (intrastrand) (31). In contrast, spontaneous depurination of the N7-guanine portion of N7G-N1A and N7G-N^6A DEB cross-links (Figure 1) results in hydrolytically stable adenine adducts containing a butanediol cross-link to free

guanine in one DNA strand and an abasic site (Ab) in the other (Supplement S-3). If produced *in vivo*, semi-depurinated interstrand cross-links may be important to DEB mutagenesis, because repair synthesis on either strand must proceed past the damaged nucleobase in the opposite strand.

In addition to interspecies differences in BD metabolism, the concentrations of DEB-DNA adduct levels in tissues of rats and mice can be affected by variations in DNA repair pathways. Experiments examining the potential roles of nucleotide excision repair and base excision repair pathways in the removal of *bis*-N7G-BD and N7G-N1A-BD adducts are currently in progress in our laboratory.

In summary, our results presented herein provide additional support to the hypothesis that DEB is the key metabolite largely responsible for the interspecies differences in sensitivity to BD-induced cancer (37,39). Our study provides a greater molecular detail of the consequences of interspecies metabolic differences by quantifying DNA-DNA lesions specific for DEB. This work also has implications for human risk assessment. While the mouse model is sometimes preferred because mice are the more sensitive species to BD-induced cancer, studies in liver microsomes suggest that mice form DEB at faster rates than both rats and humans (11). In addition, human microsomes have higher epoxide hydrolase activity than rats and mice, and therefore hydrolyze DEB more efficiently than both rat and mouse microsomes (11). Therefore, if DEB is responsible for BD-induced cancer in the mouse, a rat model of sensitivity may be more appropriate for setting limits of human exposure.

Supplementary Material

Refer to Web version on PubMed Central for supplementary material.

List of Abbreviations

BD	1,3-butadiene
bis-N7G-BD	1,4-*bis*-(guan-7-yl)-2,3-butanediol
BLQ	below the limit of quantitation
DEB	1,2,3,4-diepoxybutane
EB	3,4-epoxy-1-butene
EBD	3,4-epoxy-1,2-butanediol
EH	epoxide hydrolase
G-A	guanine-adenine
HPLC-μESI$^+$-MS/MS	liquid chromatography-microelectrospray ionization tandem mass spectrometry
HPLC-nESI$^+$-MS/MS	high performance liquid chromatography-nanoelectrospray ionization tandem mass spectrometry
N7-HEB-G	N7-(2'-hydroxy-3', 4'-epoxybut-1'-yl)-guanine
N7G-N1A-BD	1-(guan-7-yl)-4-(aden-1-yl)-2,3-butanediol
N7G-N^{6}A-BD	1-(guan-7-yl)-4-(aden-6-yl)-2,3-butanediol
pyr-Val	*N,N*-(2,3-dihydroxy-1,4-butanediyl)-valine
SD	standard deviation
SRM	selected reaction monitoring

THBG	*N7*-(2, 3, 4-trihydroxybut-1-yl)guanine

Acknowledgments

We thank Brock Matter and Peter Villalta (University of Minnesota Cancer Center) for help with developing nanospray MS methods, Bob Carlson (University of Minnesota Cancer Center) for preparing figures for this manuscript, as well as Gunnar Boysen and Nadia Christova-Georgieva (UNC) for their helpful comments on the finished manuscript. This work was supported by grants from the National Cancer Institute (C.A. 100670), the National Institute of Environmental Health Sciences (ES 12689), the Health Effects Institute (Agreement 05-12), and the American Chemistry Council (OLF-163.0).

References

1. White WC. Butadiene production process overview. Chem Biol Interact 2007;166:10–14. [PubMed: 17324391]
2. Pelz N, Dempster NM, Shore PR. Analysis of low molecular weight hydrocarbons including 1,3-butadiene in engine exhaust gases using an aluminum oxide porous-layer open-tubular fused-silica column. J Chromatogr Sci 1990;28:230–235. [PubMed: 1704381]
3. Hecht SS. Tobacco smoke carcinogens and lung cancer. J Natl Cancer Inst 1999;91:1194–1210. [PubMed: 10413421]
4. Stayner LT, Dankovic DA, Smith RJ, Gilbert SJ, Bailer AJ. Human cancer risk and exposure to 1,3-butadiene--a tale of mice and men. Scand J Work Environ Health 2000;26:322–330. [PubMed: 10994798]
5. Ward JB Jr, Ammenheuser MM, Bechtold WE, Whorton EB Jr, Legator MS. hprt mutant lymphocyte frequencies in workers at a 1,3-butadiene production plant. Environ Health Perspect 1994;102:79–85. [PubMed: 7698091]
6. Melnick RL, Huff J, Chou BJ, Miller RA. Carcinogenicity of 1,3-butadiene in C57BL/6 × C3H F1 mice at low exposure concentrations. Cancer Res 1990;50:6592–6599. [PubMed: 2208121]
7. Melnick RL, Shackelford CC, Huff J. Carcinogenicity of 1,3-butadiene. Environ Health Perspect 1993;100:227–236. [PubMed: 8354171]
8. Melnick RL, Huff JE. 1,3-Butadiene induces cancer in experimental animals at all concentrations from 6.25 to 8000 parts per million. IARC Sci Publ 1993:309–322. [PubMed: 8070878]
9. Malvoisin E, Roberfroid M. Hepatic microsomal metabolism of 1,3-butadiene. Xenobiotica 1982;12:137–144. [PubMed: 7090423]
10. Himmelstein MW, Turner MJ, Asgharian B, Bond JA. Metabolism of 1,3-butadiene: inhalation pharmacokinetics and tissue dosimetry of butadiene epoxides in rats and mice. Toxicology 1996;113:306–309. [PubMed: 8901914]
11. Krause RJ, Elfarra AA. Oxidation of butadiene monoxide to meso- and (+/−)-diepoxybutane by cDNA-expressed human cytochrome P450s and by mouse, rat, and human liver microsomes: evidence for preferential hydration of meso-diepoxybutane in rat and human liver microsomes. Arch Biochem Biophys 1997;337:176–184. [PubMed: 9016811]
12. Cochrane JE, Skopek TR. Mutagenicity of butadiene and its epoxide metabolites: I. Mutagenic potential of 1,2-epoxybutene, 1,2,3,4-diepoxybutane and 3,4-epoxy-1,2-butanediol in cultured human lymphoblasts. Carcinogenesis 1994;15:713–717. [PubMed: 8149485]
13. Park S, Tretyakova N. Structural Characterization of the Major DNA-DNA Cross-Link of 1,2,3,4-Diepoxybutane. Chem Res Toxicol 2004;17:129–136. [PubMed: 14966999]
14. Zhang XY, Elfarra AA. Reaction of 1,2,3,4-diepoxybutane with 2'-deoxyguanosine: initial products and their stabilities and decomposition patterns under physiological conditions. Chem Res Toxicol 2005;18:1316–1323. [PubMed: 16097805]
15. Himmelstein MW, Acquavella JF, Recio L, Medinsky MA, Bond JA. Toxicology and epidemiology of 1,3-butadiene. Crit Rev Toxicol 1997;27:1–108. [PubMed: 9115622]

16. Tretyakova NY, Sangaiah R, Yen TY, Swenberg JA. Synthesis, characterization, and *in vitro* quantitation of N-7-guanine adducts of diepoxybutane. Chem Res Toxicol 1997;10:779–785. [PubMed: 9250412]

17. Park S, Hodge J, Anderson C, Tretyakova NY. Guanine-adenine cross-linking by 1,2,3,4-diepoxybutane: potential basis for biological activity. Chem Res Toxicol 2004;17:1638–1651. [PubMed: 15606140]

18. Goggin M, Anderson C, Park S, Swenberg J, Walker V, Tretyakova N. Quantitative high-performance liquid chromatography-electrospray ionization-tandem mass spectrometry analysis of the adenine-guanine cross-links of 1,2,3,4-diepoxybutane in tissues of butadiene-exposed B6C3F1 mice. Chem Res Toxicol 2008;21:1163–1170. [PubMed: 18442269]

19. Owen PE, Glaister JR, Gaunt IF, Pullinger DH. Inhalation toxicity studies with 1,3-butadiene. 3. Two year toxicity/carcinogenicity study in rats. Am Ind Hyg Assoc J 1987;48:407–413. [PubMed: 3591659]

20. Jelitto B, Vangala RR, Laib RJ. Species differences in DNA damage by butadiene: role of diepoxybutane. Arch Toxicol Suppl 1989;13:246–249. [PubMed: 2774939]

21. Henderson RF, Barr EB, Belinsky SA, Benson JM, Hahn FF, Menache MG. 1,3-butadiene: cancer, mutations, and adducts. Part I: Carcinogenicity of 1,2,3,4-diepoxybutane. Res Rep Health Eff Inst 2000:11–43. [PubMed: 10925838]

22. Henderson RF, Thornton-Manning JR, Bechtold WE, Dahl AR. Metabolism of 1,3-butadiene: species differences. Toxicology 1996;113:17–22. [PubMed: 8901878]

23. Thornton-Manning JR, Dahl AR, Bechtold WE, Griffith WC Jr, Henderson RF. Disposition of butadiene monoepoxide and butadiene diepoxide in various tissues of rats and mice following a low-level inhalation exposure to 1,3-butadiene. Carcinogenesis 1995;16:1723–1731. [PubMed: 7634396]

24. Boysen G, Georgieva NI, Upton PB, et al. Analysis of diepoxide-specific cyclic N-terminal globin adducts in mice and rats after inhalation exposure to 1,3-butadiene. Cancer Res 2004;64:8517–8520. [PubMed: 15574756]

25. Filser JG, Hutzler C, Meischner V, Veereshwarayya V, Csanady GA. Metabolism of 1,3-butadiene to toxicologically relevant metabolites in single-exposed mice and rats. Chem Biol Interact 2007;166:93–103. [PubMed: 16616907]

26. Kligerman AD, DeMarini DM, Doerr CL, Hanley NM, Milholland VS, Tennant AH. Comparison of cytogenetic effects of 3,4-epoxy-1-butene and 1,2:3, 4-diepoxybutane in mouse, rat and human lymphocytes following in vitro G0 exposures. Mutat Res 1999;439:13–23. [PubMed: 10029668]

27. Kligerman AD, Hu Y. Some insights into the mode of action of butadiene by examining the genotoxicity of its metabolites. Chem Biol Interact. 2006 Epub ahead of print 4/18/2006:

28. Koc H, Tretyakova NY, Walker VE, Henderson RF, Swenberg JA. Molecular dosimetry of N-7 guanine adduct formation in mice and rats exposed to 1,3-butadiene. Chem Res Toxicol 1999;12:566–574. [PubMed: 10409395]

29. Swenberg JA, Boysen G, Georgieva N, Bird MG, Lewis RJ. Future directions in butadiene risk assessment and the role of cross-species internal dosimetry. Chem Biol Interact 2007;166:78–83. [PubMed: 17343837]

30. Goggin M, Loeber R, Park S, Walker V, Wickliffe J, Tretyakova N. HPLC-ESI+-MS/MS analysis of N7-guanine-N7-guanine DNA cross-links in tissues of mice exposed to 1,3-butadiene. Chem Res Toxicol 2007;20:839–847. [PubMed: 17455958]

31. Park S, Anderson C, Loeber R, Seetharaman M, Jones R, Tretyakova N. Interstrand and intrastrand DNA-DNA cross-linking by 1,2,3,4-diepoxybutane: role of stereochemistry. J Am Chem Soc 2005;127:14355–14365. [PubMed: 16218630]

32. Singer, B.; Grunberger, D. Molecular Biology of Mutagens and Carcinogens. New York and London: Plenum Press; 1983.

33. Tretyakova NY, Lin YP, Upton PB, Sangaiah R, Swenberg JA. Macromolecular adducts of butadiene. Toxicology 1996;113:70–76. [PubMed: 8901884]

34. Koivisto P, Adler ID, Pacchierotti F, Peltonen K. DNA adducts in mouse testis and lung after inhalation exposure to 1,3-butadiene. Mutat Res 1998;397:3–10. [PubMed: 9463547]

35. Oesch-Bartlomowicz B, Padma PR, Becker R, et al. Differential modulation of CYP2E1 activity by cAMP-dependent protein kinase upon Ser129 replacement. Exp Cell Res 1998;242:294–302. [PubMed: 9665827]
36. Boysen G, Scarlett CO, Temple B, et al. Identification of covalent modifications in P450 2E1 by 1,2-epoxy-3-butene in vitro. Chem Biol Interact 2007;166:170–175. [PubMed: 17298833]
37. Boysen G, Georgieva NI, Upton PB, Walker VE, Swenberg JA. *N*-terminal globin adducts as biomarkers for formation of butadiene derived epoxides. Chem Biol Interact 2007;166:84–92. [PubMed: 17084829]
38. Swenberg JA, Fryar-Tita E, Jeong YC, et al. Biomarkers in toxicology and risk assessment: informing critical dose-response relationships. Chem Res Toxicol 2008;21:253–265. [PubMed: 18161944]
39. Thornton-Manning JR, Dahl AR, Bechtold WE, Henderson RF. Gender and species differences in the metabolism of 1,3-butadiene to butadiene monoepoxide and butadiene diepoxide in rodents following low-level inhalation exposures. Toxicology 1996;113:322–325. [PubMed: 8901918]
40. Hayes RB, Zhang L, Yin S, et al. Genotoxic markers among butadiene polymer workers in China. Carcinogenesis 2000;21:55–62. [PubMed: 10607734]
41. Albertini RJ, Sram RJ, Vacek PM, et al. Molecular epidemiological studies in 1,3-butadiene exposed Czech workers: female-male comparisons. Chem Biol Interact 2007;166:63–77. [PubMed: 16949064]
42. Millard JT, White MM. Diepoxybutane cross-links DNA at 5'-GNC sequences. Biochemistry 1993;32:2120–2124. [PubMed: 8448170]
43. Millard JT, Wilkes EE. Diepoxybutane and diepoxyoctane interstrand cross-linking of the 5S DNA nucleosomal core particle. Biochemistry 2001;40:10677–10685. [PubMed: 11524013]
44. Millard JT, Hanly TC, Murphy K, Tretyakova N. The 5'-GNC site for DNA interstrand cross-linking is conserved for diepoxybutane stereoisomers. Chem Res Toxicol 2006;19:16–19. [PubMed: 16411651]
45. Lawley PD, Brookes P. Interstrand cross-linking of DNA by difunctional alkylating agents. J Mol Biol 1967;25:143–160. [PubMed: 5340530]

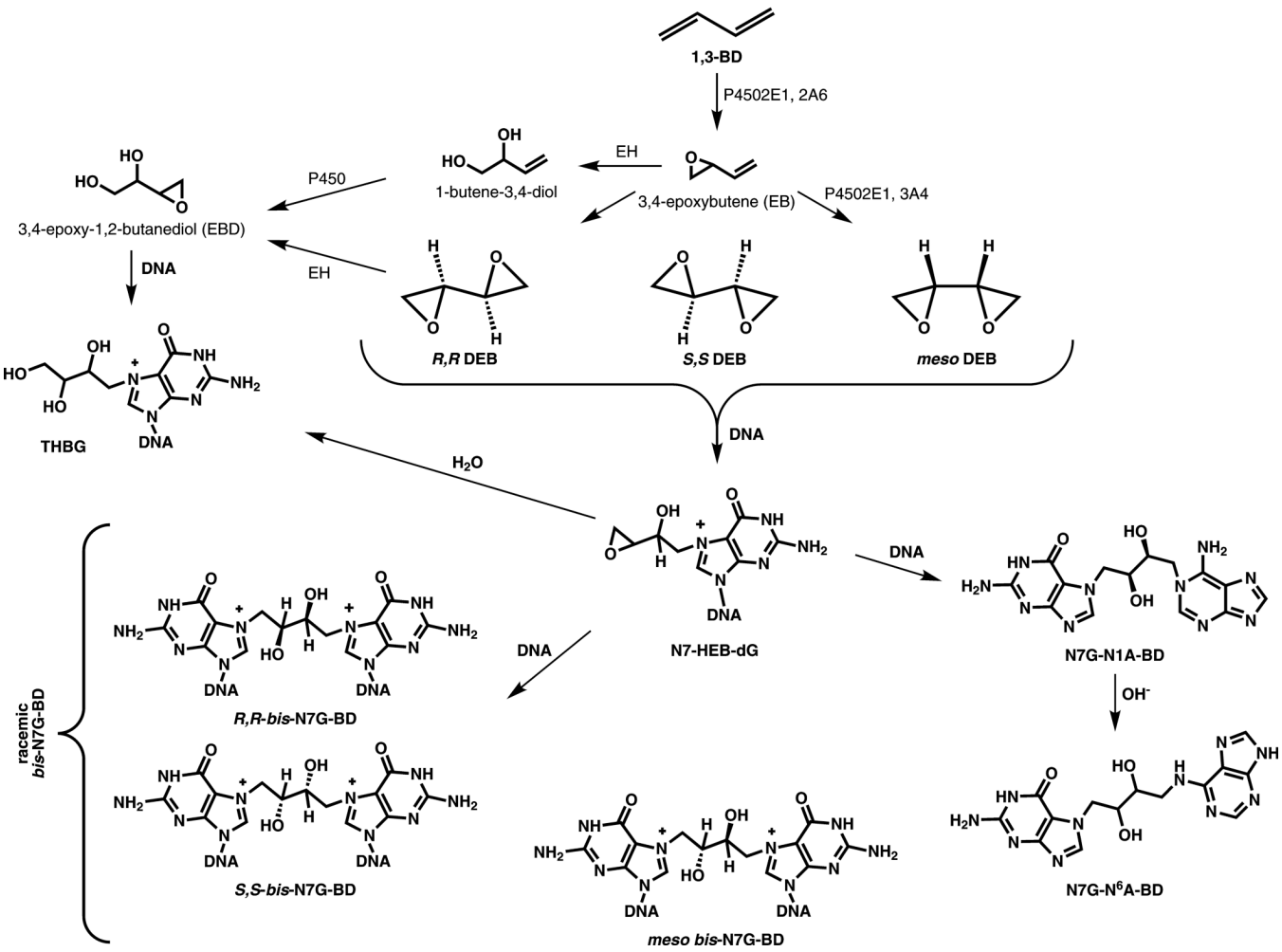

Figure 1.
Metabolic activation of 1,3-butadiene to reactive electrophiles and the formation of DNA adducts.

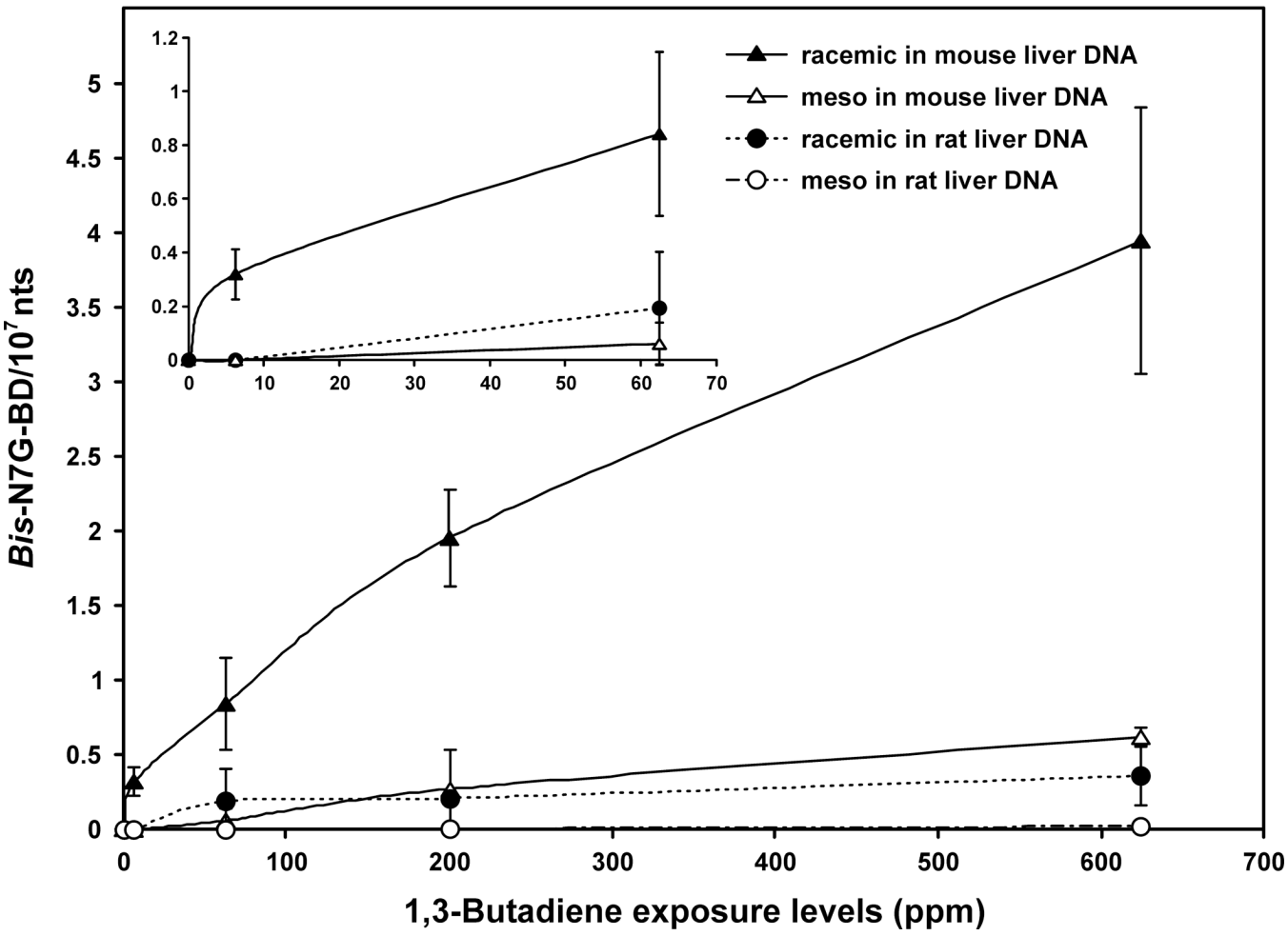

Figure 2.

Dose dependent formation of *bis*-N7G-BD in liver DNA of female B6C3F1 mice and female F344 rats exposed to 1,3-butadiene by inhalation. Animals were exposed to 0, 6.25, 62.5, 200, or 625 ppm BD for 2 weeks. Closed triangle = racemic *bis*-N7G-BD in mouse liver DNA, open triangles = *meso bis*-N7G-BD in mouse liver. Closed circles = racemic *bis*-N7G-BD in rat liver DNA, open circles = *meso bis*-N7G-BD in rat liver DNA.

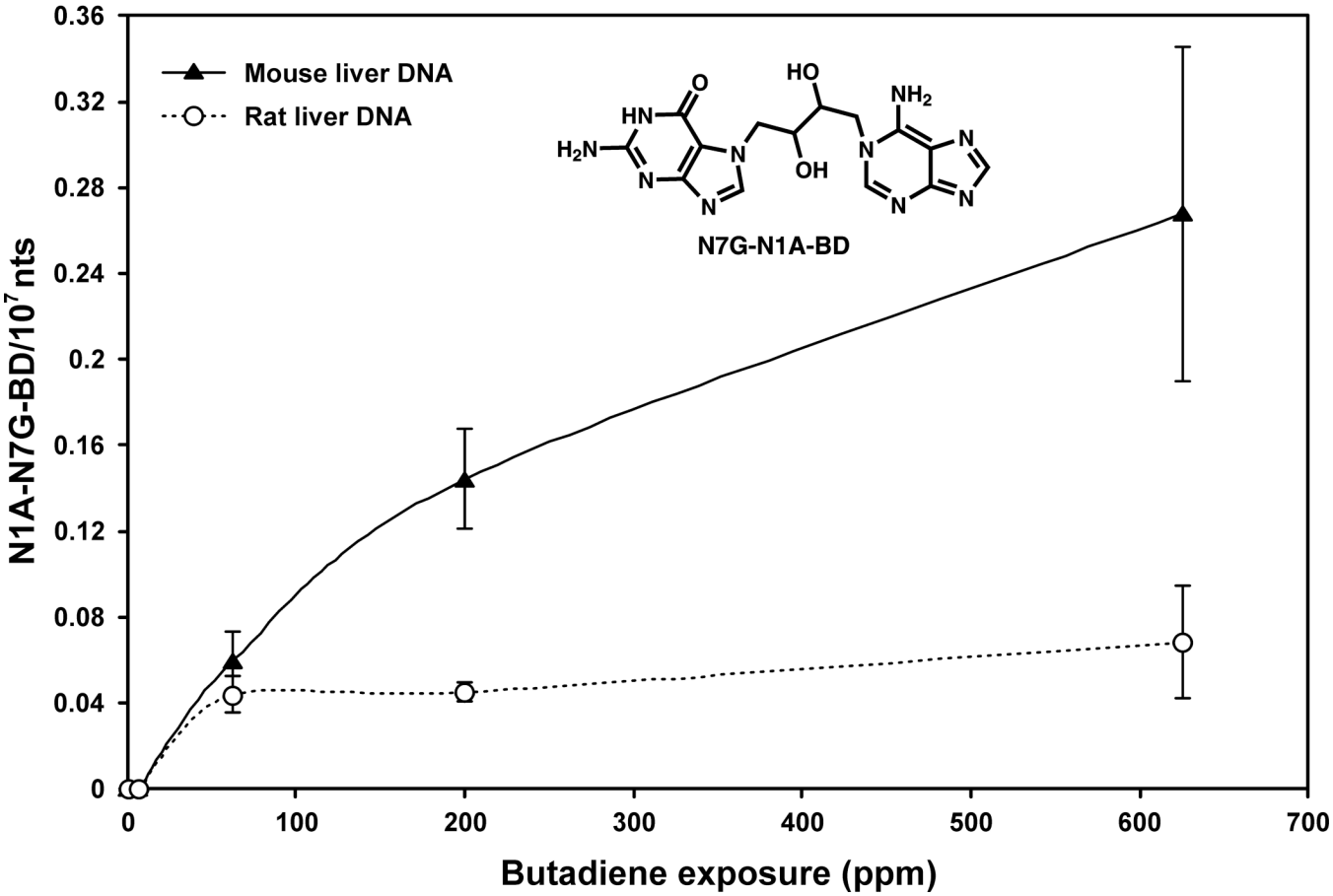

Figure 3.

Dose dependent formation of N7G-N1A-BD/N7G-N^{6}A-BD in liver DNA of female B6C3F1 mice and female F344 rats exposed to 1,3-butadiene by inhalation (same animals as figure 1). Closed triangles = N7G-N1A-BD + N7G-N^{6}A-BD in mouse DNA and closed circles = N7G-N1A-BD + N7G-N^{6}A-BD in rat liver DNA.

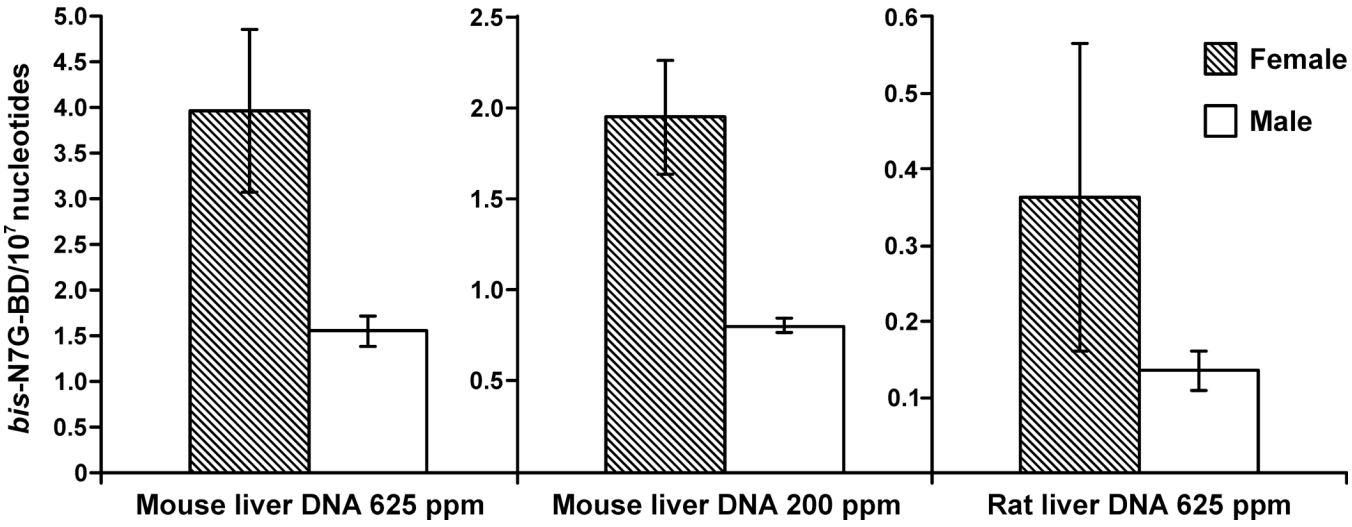

Figure 4.

Gender differences in the formation of racemic *bis*-N7G-BD in B6C3F1 mice and F344 rats exposed to 625 ppm BD, and mice exposed to 200 ppm BD by inhalation for 2 weeks. *Differences between female and male mice at 625 ppm and 200 ppm BD is statistically significant, p-values = 0.014 and 0.006. Difference between female and male rats is not statistically significant, p-value = 0.19.

Table 1

Tissue differences in the formation of racemic *bis*-N7G-BD in female B6C3F1 mice and female F344 rats exposed to 625 ppm BD by inhalation for 2 weeks.

Tissue	Racemic *bis*-N7G-BD per 10^7 nts in mouse	Racemic *bis*-N7G-BD per 10^7 nts in rat
Liver (N = 4)	3.95 ± 0.89	0.36 ± 0.23
Lung (N = 4)	1.35 ± 0.12	0.30 ± 0.01
Kidney (N = 4)	1.10 ± 0.13	0.14 ± 0.05
Brain (N = 4)	0.38 ± 0.15	0.24 ± 0.06
Thymus (N = 4)	1.15 ± 0.26	0.21 ± 0.06

Table 2

Bis-N7G-BD adduct levels in mouse liver DNA per unit dose of 1,3-butadiene. ND, not detected.

BD exposure (ppm)	Racemic *bis*-N7G-BD adducts /10^6 nts/ppm BD in mouse liver DNA	Racemic *bis*-N7G-BD adducts /10^6 nts/ppm BD in rat liver DNA
0	ND	ND
6.25	0.51	ND
62.5	0.13	0.031
200	0.098	0.010
625	0.063	0.006